CHAPTER IV
RESULTS AND DISCUSSION

4.1 Characterization of Benzoxazine Monomers

3,4-dihydro-3-methyl-6-methyl-2H-1,3-benzoxazine (1), 3,4-dihydro-3-methyl-6,8-methyl-2H-1,3-benzoxazine (2), and 3,4-dihydro-3-methyl-6-ethyl-2H-1,3-benzoxazine (3) (see Scheme 3.2) were synthesized from *p*-cresol, 2,4-dimethylphenol and ethylphenol, respectively, by the reaction with paraformaldehyde and methylamine in the molar ratio of 1:2:1. The products were characterized as follows.

4.1.1 Structural Characterization of 3,4-dihydro-3-methyl-6-methyl-2H-1,3-benzoxazine (1)

Yield : 67.64%. R_f (TLC, EtOAc:$CHCl_3$ (3:2 v/v)) 0.58. FTIR (KBr, in cm^{-1}): 1501 (oxazine), 1251 (C-N stretching), 1286,1118,1030 (C-O-C stretching), 815,857 (1,2,4 substituted). ^{1}H-NMR (200MHz, $CDCl_3$, δ values in ppm from TMS): 2.33 (3H, s, Ar-CH_3), 2.68 (3H, s, N-CH_3), 4.00 (2H, s, Ar-CH_2-N), 4.84 (2H, s, O-CH_2-N), 6.76-6.79 (1H, d, Ar-H), 6.84 (1H, s, Ar-H), 6.98-7.01 (1H, d, Ar-H).

4.1.2 Structural Characterization of 3,4-dihydro-3-methyl-6,8-methyl-2H-1,3-benzoxazine (2)

Yield : 82.99%. R_f (TLC, EtOAc:$CHCl_3$ (3:2 v/v)) 0.60. FTIR (KBr, in cm^{-1}): 1485 (oxazine), 1258 (C-N stretching), 1287,1149,1059,1035 (C-O-C stretching), 850 (1,2,3,5 substituted). ^{1}H-NMR (200MHz, $CDCl_3$, δ values in ppm from TMS): 2.22 (3H, s, Ar-CH_3), 2.27 (3H, s, Ar-CH_3), 2.59 (3H, s, N-CH_3), 3.93 (2H, s, Ar-CH_2-N), 4.82 (2H, s, O-CH_2-N), 6.65 (1H, s, Ar-H), 6.86 (1H, s, Ar-H).

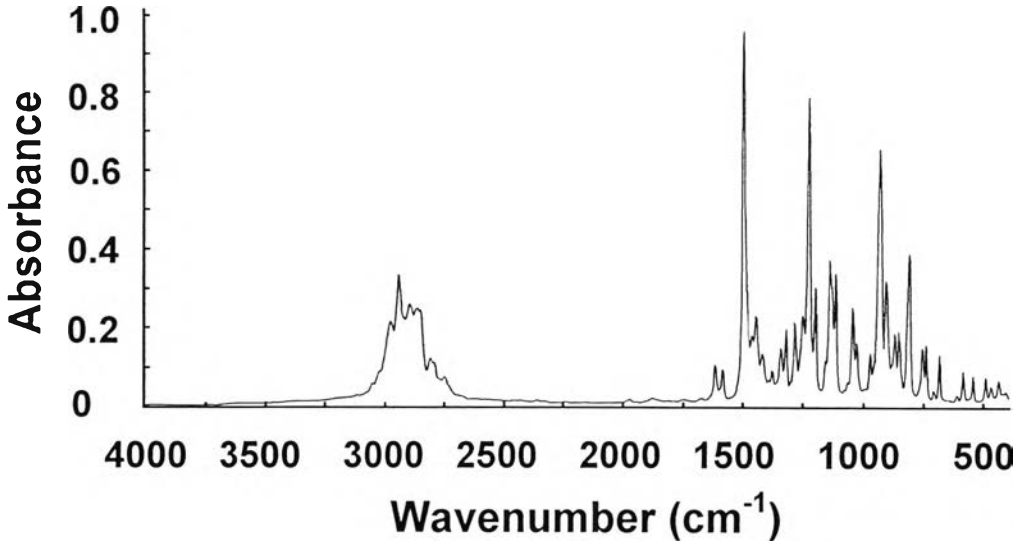

Figure 4.1 FTIR spectrum of (1).

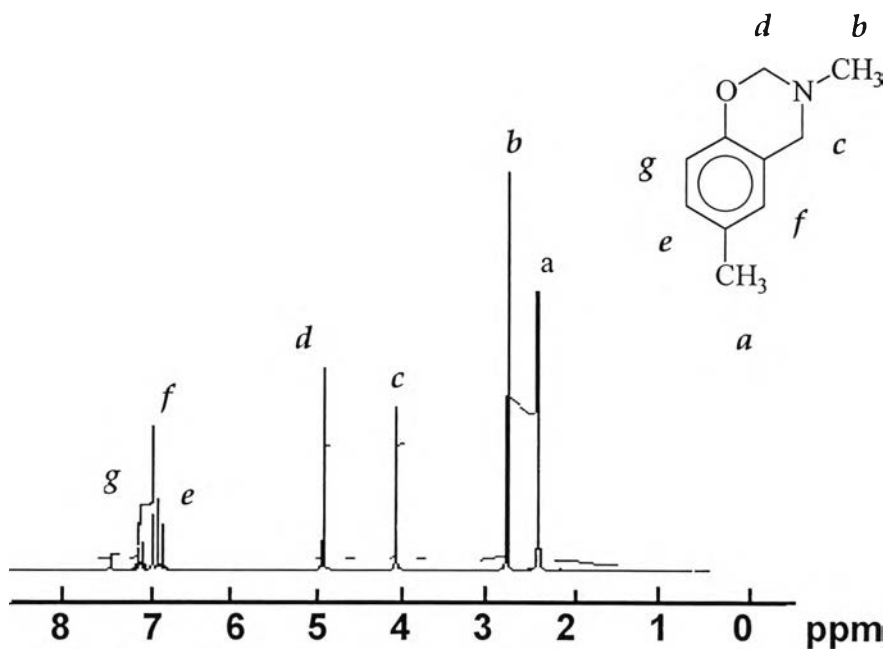

Figure 4.2 ^{1}H-NMR spectrum of (1).

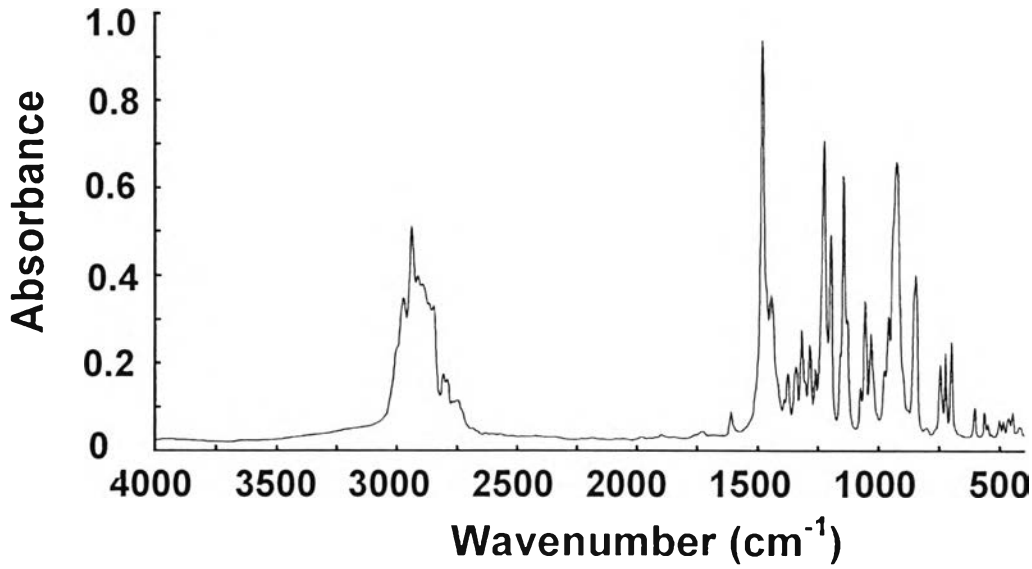

Figure 4.3 FTIR spectrum of (2).

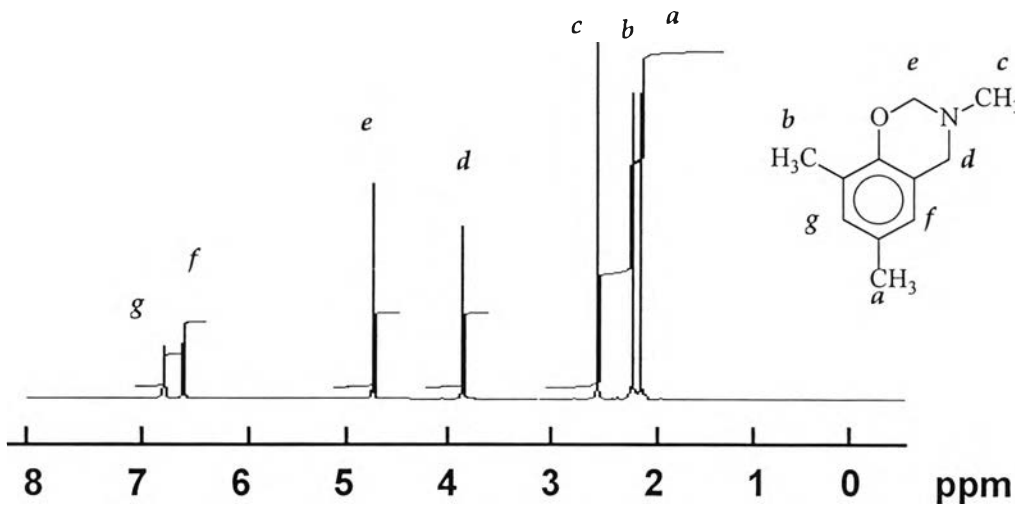

Figure 4.4 ^{1}H-NMR spectrum of (2).

4.1.3 Structural Characterization of 3,4-dihydro-3-methyl-6-ethyl-2H-1,3-benzoxazine (3)

Yield : 88.62%. R_f(TLC, EtOAc:$CHCl_3$ (3:2 v/v) 0.57. FTIR (KBr, in cm^{-1}): 1499 (oxazine), 1229 (C-N stretching), 1286,1118,1029 (C-O-C stretching), 822,858 (1,2,4 substituted). ^{1}H-NMR (200MHz, $CDCl_3$, δ values in ppm from TMS): 1.98 (3H, t, Ar-CH_2-CH_3), 2.54 (3H, m, Ar-CH_2-CH_3), 2.58 (3H, s, N-CH_3), 3.91 (2H, s, Ar-CH_2-N), 4.74 (2H, s, O-CH_2-N), 6.70 (1H, s, Ar-H), 6.76 (1H, s, Ar-H), 6.93 (1H, s, Ar-H).

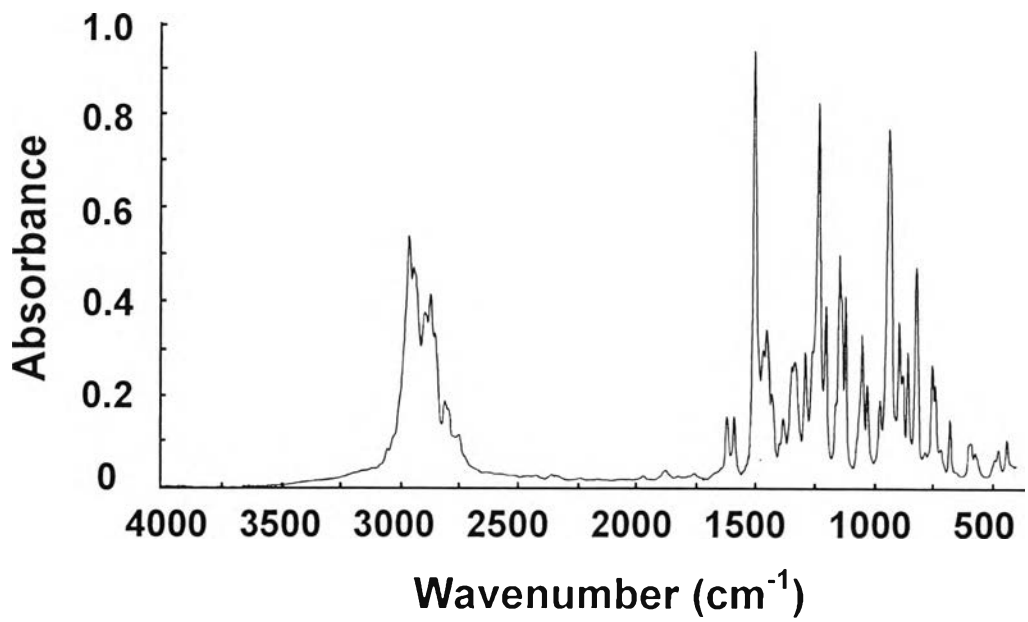

Figure 4.5 FTIR spectrum of (3).

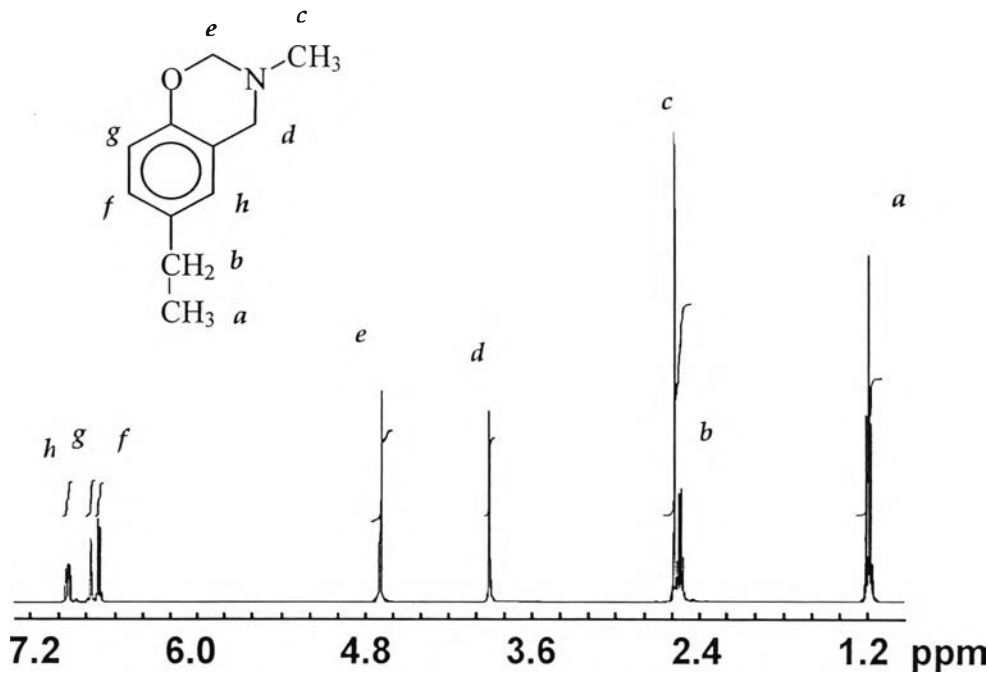

Figure 4.6 ^{1}H-NMR spectrum of (3).

4.2 Characterization of Benzoxazine Dimers

N,N-Bis (5-methyl-2-hydroxybenzyl) methylamine (4), N,N-Bis (3,5-dimethyl-2-hydroxybenzyl) methylamine (5), and N,N-Bis (5-ethyl-2-hydroxy benzyl) methylamine (6) (see Scheme 3.4) were recrystallized in 80:20 hexane : THF. The products were characterized as follows.

4.2.1 Structural Characterization of N,N-Bis (5-methyl-2-hydroxy benzyl) methylamine (4)

Yield : 36.23%. R_f (TLC, EtOAc:$CHCl_3$ (3:2 v/v)) 0.48. FTIR (KBr, in cm^{-1}): 3279 (O-H stretching), 1423 (N-CH_3 stretching), 1207 (C-N-C asym. stretching), 850,825 (C-N-C sym. Stretching). ^{1}H-NMR (200MHz, $CDCl_3$, δ values in ppm from TMS): 2.23 (6H, s, Ar-CH_3), 2.23 (3H, s, N-CH_3), 3.69 (4H, s, Ar-CH_2-N), 6.7 (2H, d, Ar-H), 6.83 (2H, s, Ar-H), 6.86 (2H, d, Ar-H).

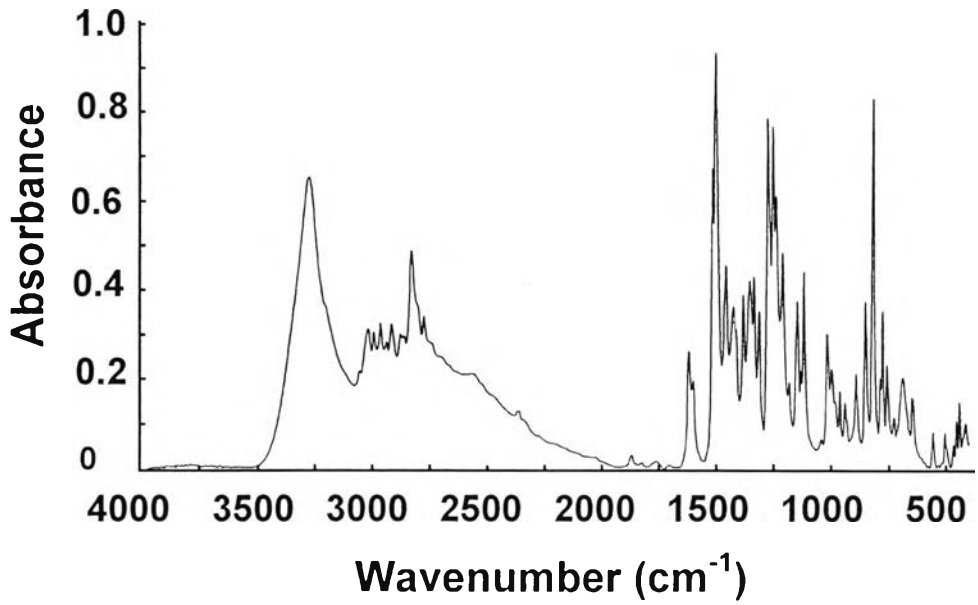

Figure 4.7 FTIR spectrum of (4).

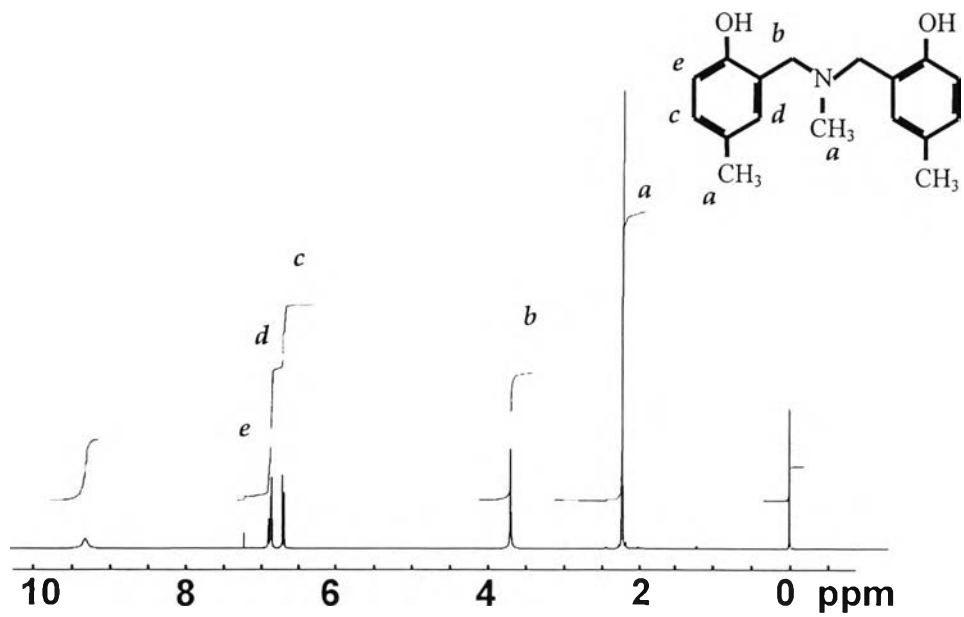

Figure 4.8 ^{1}H-NMR spectrum of (4).

4.2.2 Structural Characterization of N,N-Bis (3,5-dimethyl-2-hydroxybenzyl) methylamine (5)

Yield : 36.49%. R_f (TLC, EtOAc:$CHCl_3$ (3:2 v/v)) 0.67. FTIR (KBr, in cm^{-1}): 3396 (O-H stretching), 1426 (N-CH_3 stretching), 1203 (C-N-C asym. stretching), 855,846 (C-N-C sym. Stretching). ^{1}H-NMR (200MHz, $CDCl_3$, δ values in ppm from TMS): 2.22 (12H, s, Ar-CH_3), 2.25 (3H, s, N-CH_3), 3.68 (4H, s, Ar-CH_2-N), 6.72 (2H, s, Ar-H), 6.81 (2H, s, Ar-H).

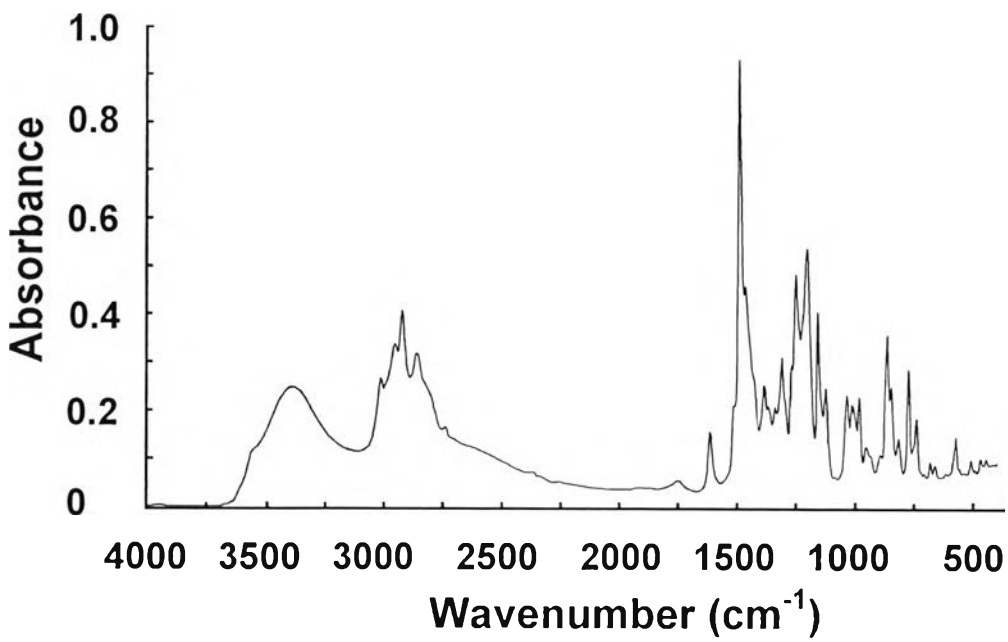

Figure 4.9 FTIR spectrum of (5).

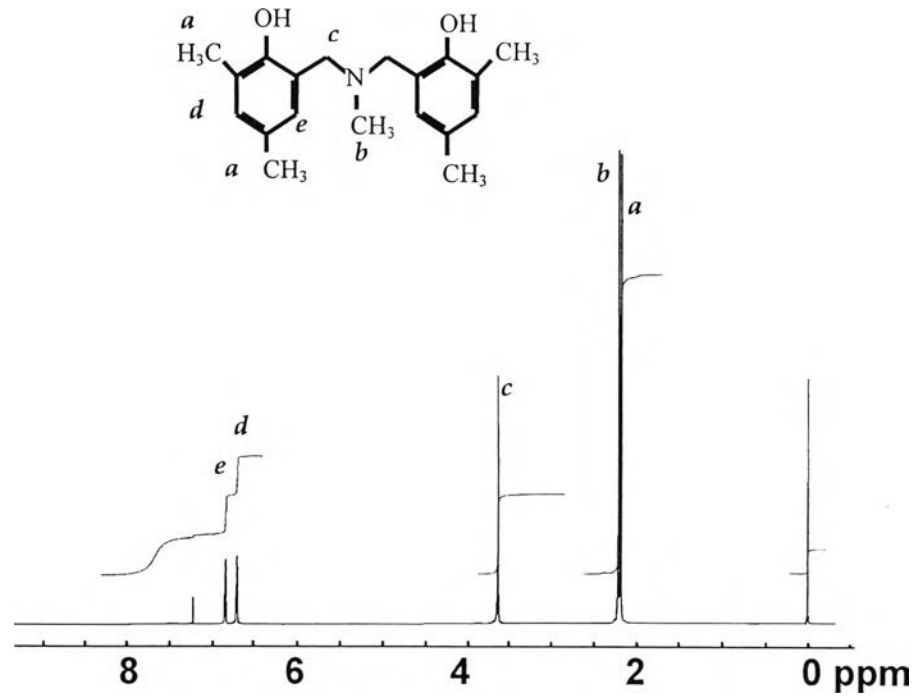

Figure 4.10 ^{1}H-NMR spectrum (5).

4.2.3 Structural Characterization of N,N-Bis (5-ethyl-2-hydroxy benzyl) methylamine (6)

Yield : 13.45%. R_f (TLC, EtOAc:$CHCl_3$ (3:2 v/v)) 0.45. FTIR (KBr, in cm^{-1}): 3301 (O-H stretching), 1437 (N-CH_3 stretching), 1208 (C-N-C asym. stretching), 847,822 (C-N-C sym. Stretching); (C-N stretching). ^{1}H-NMR (200MHz, $CDCl_3$, δ values in ppm from TMS): 1.17 (6H, t, Ar-CH_2-CH_3), 2.25 (3H, s, N-CH_3), 2.54 (4H, m, Ar-CH_2-CH_3), 3.72 (4H, s, Ar-CH_2-N), 6.73 (2H, d, Ar-H), 6.87 (2H, s, Ar-H), 6.94 (2H, d, Ar-H).

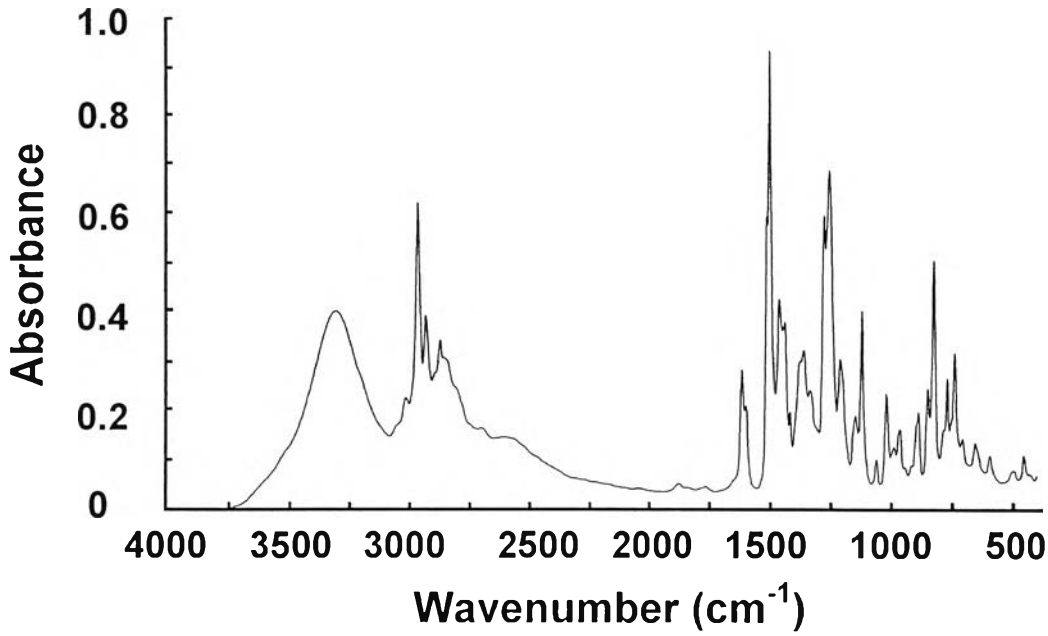

Figure 4.11 FTIR spectrum of (6).

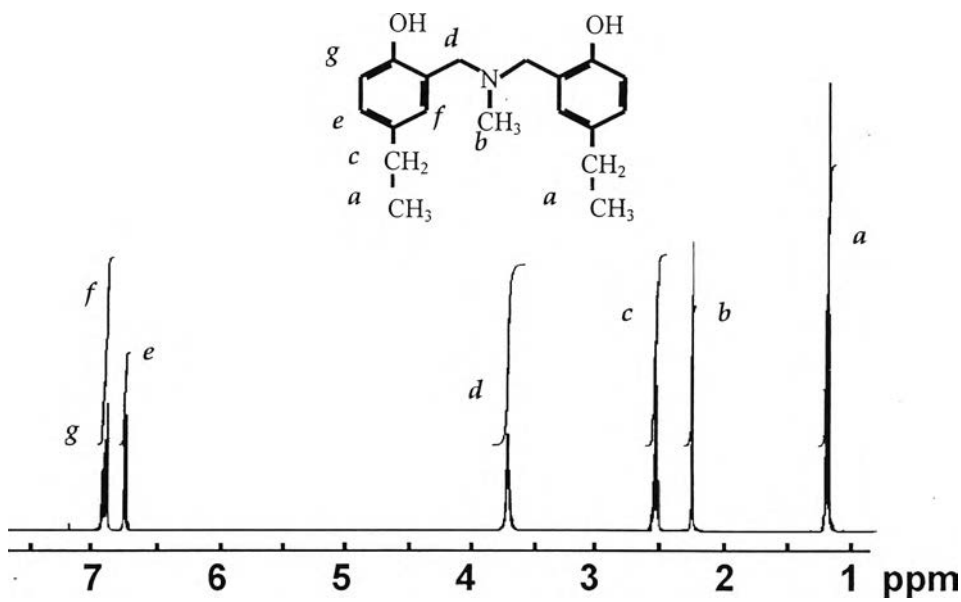

Figure 4.12 ^{1}H-NMR spectrum (6).

4.3 Characterization of Benzoxazine Dimer Derivatives

The benzoxazine dimer derivatives, N,N-Bis (5-methyl-2-benzoylben zyl) methylamine (7), N,N-Bis (5-methyl-2-acetylbenzyl) methylamine (8), N,N-Bis (3,5-dimethyl-2-benzoylbenzyl) methylamine (9), N,N-Bis (3,5-dime thyl-2-acetylbenzyl) methylamine (10), N,N-Bis (5-ethyl-2-benzoylbenzyl) methylamine (11), and N,N-Bis (5-ethyl-2-acetylbenzyl) methylamine (12), were characterized as follows.

4.3.1 Structural Characterization of N,N-Bis (5-methyl-2-benzoyl benzyl) methylamine (7)

Yield : 94.2%. R_f (TLC, MeOH:$CHCl_3$ (1:19 v/v)) 0.95. FTIR (KBr, in cm^{-1}): 1738 (-COO-); 1452 (N-CH_3 stretching). ^{1}H-NMR (200MHz, $CDCl_3$, δ values in ppm from TMS): 2.12 (3H, s, N-CH_3), 2.35 (6H, s, Ar-CH_3), 3.47 (4H, s, Ar-CH_2-N), 6.97 (2H, d, Ar-H), 6.97 (2H, s, Ar-H), 7.1 (2H, d, Ar-H), 7.48 (4H, t, Ar-H), 7.65 (2H, t, Ar-H), 8.20 (4H, d, Ar-H).

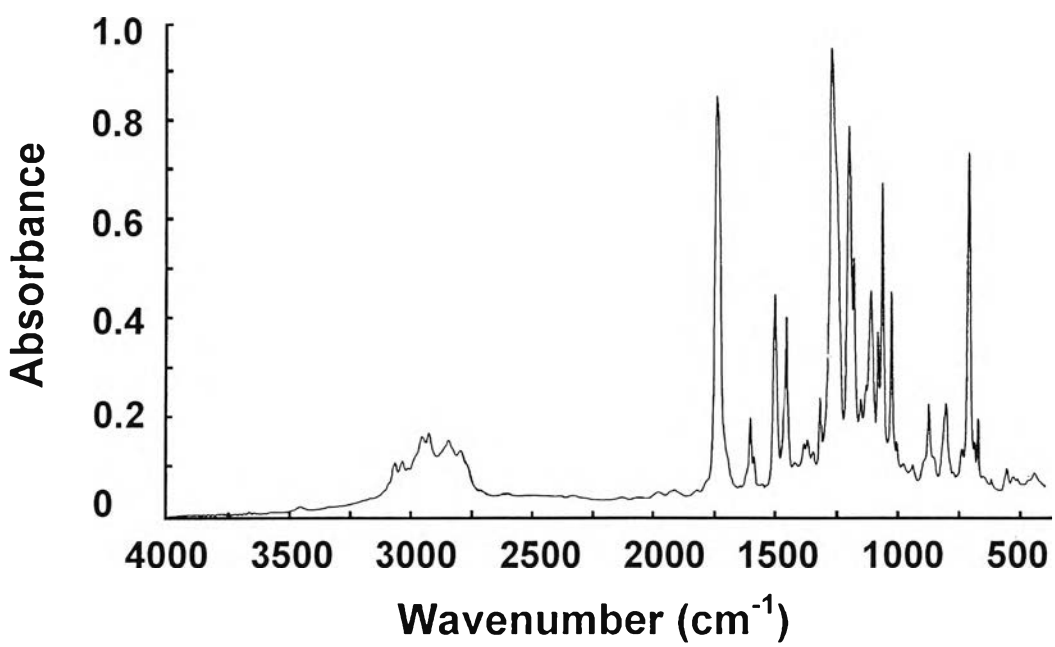

Figure 4.13 FTIR spectrum of (7).

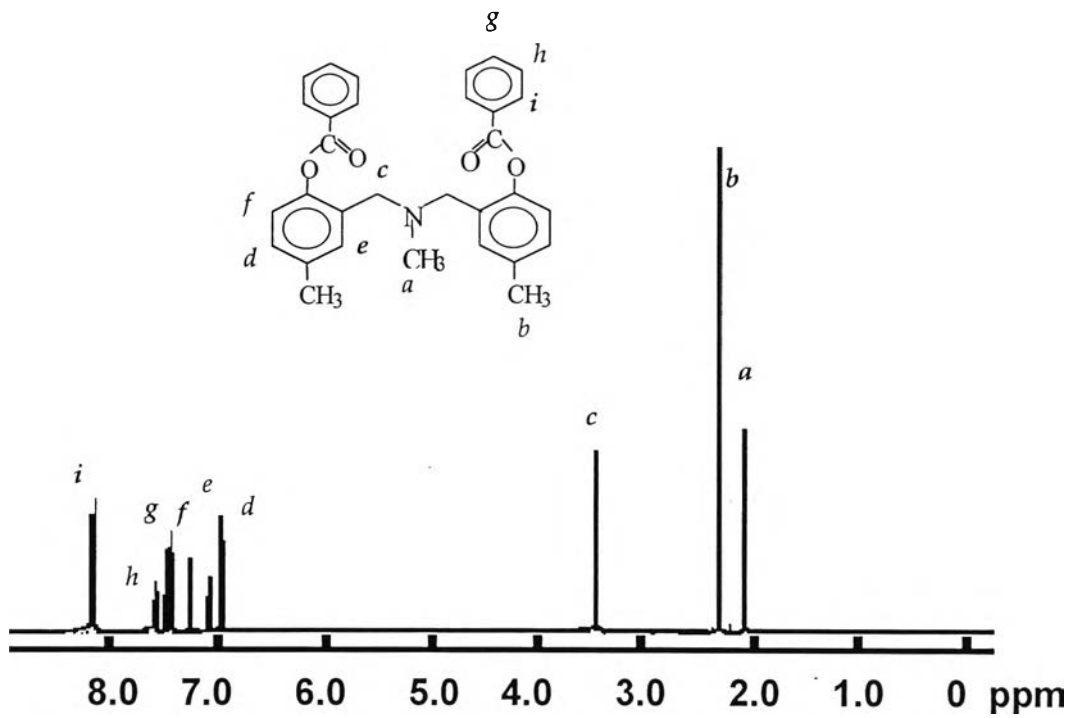

Figure 4.14 ^{1}H-NMR spectrum of (7).

4.3.2 Structural Characterization of N,N-Bis (5-methyl-2-acetyl benzyl) methylamine (8)

Yield : 90.9%. R_f (TLC, MeOH:$CHCl_3$ (1:19 v/v)) 0.94. FTIR (KBr, in cm^{-1}): 1762 (-COO-); 1480 (N-CH_3 stretching).

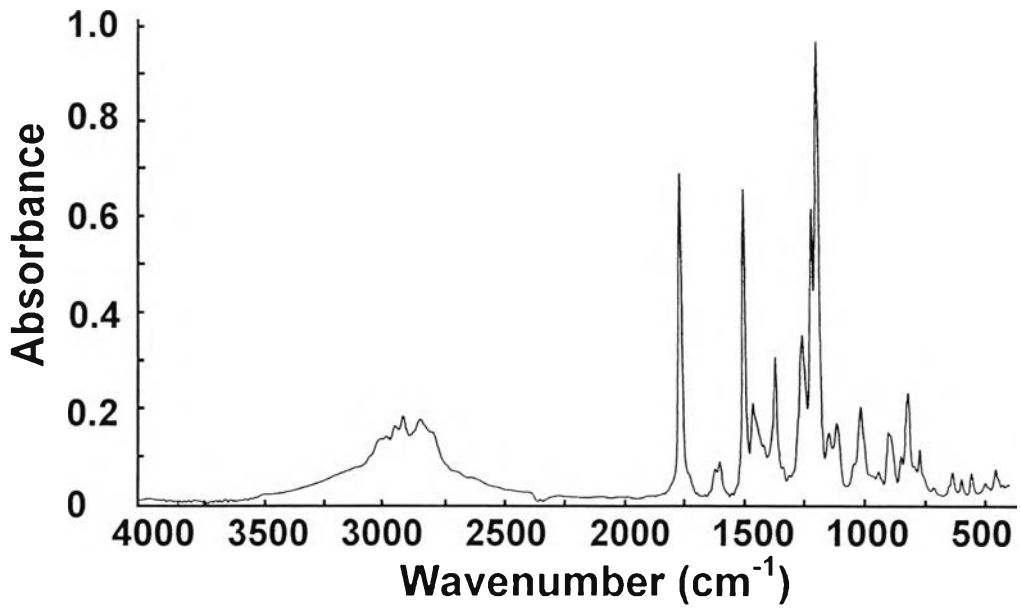

Figure 4.15 FTIR spectrum of (8).

4.3.3 Structural Characterization of N,N-Bis (3,5-dimethyl-2-benzoyl benzyl) methylamine (9)

Yield : 80.7%. R_f (TLC, MeOH:$CHCl_3$ (1:19 v/v)) 0.96. FTIR (KBr, in cm^{-1}): 1736 (-COO-); 1452 (N-CH_3 stretching). ^{1}H-NMR (200MHz, $CDCl_3$, δ values in ppm from TMS): 2.10 (6H, s, Ar-CH_3), 2.20 (3H, s, N-CH_3), 2.22 (6H, s, Ar-CH_3), 3.55 (4H, s, Ar-CH_2-N), 6.98 (2H, s, Ar-H), 7.12 (2H, s, Ar-H), 7.49 (4H, t, Ar-H), 7.62 (2H, t, Ar-H), 8.16 (4H, d, Ar-H).

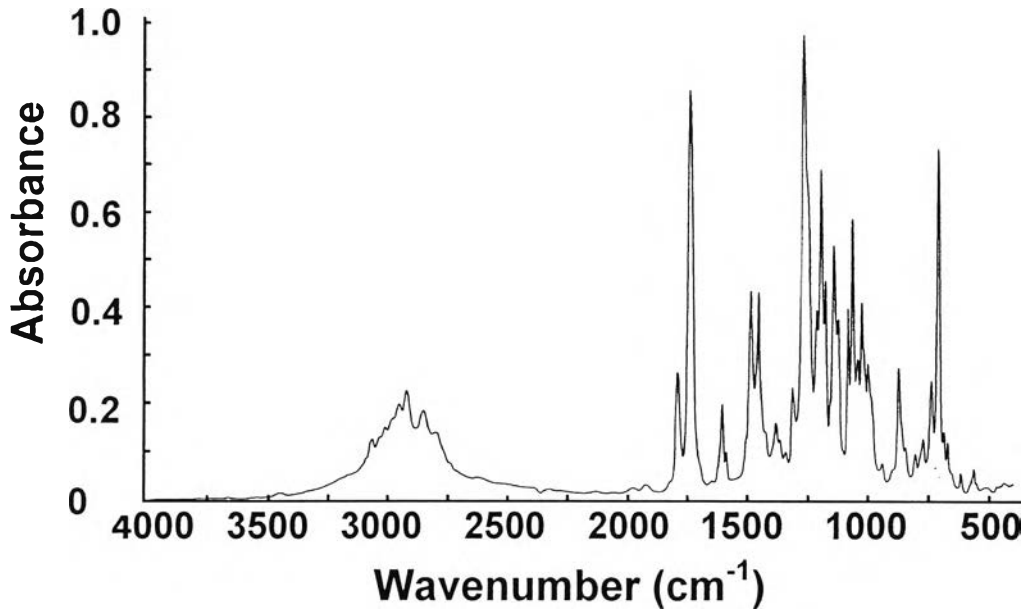

Figure 4.16 FTIR spectrum of (9).

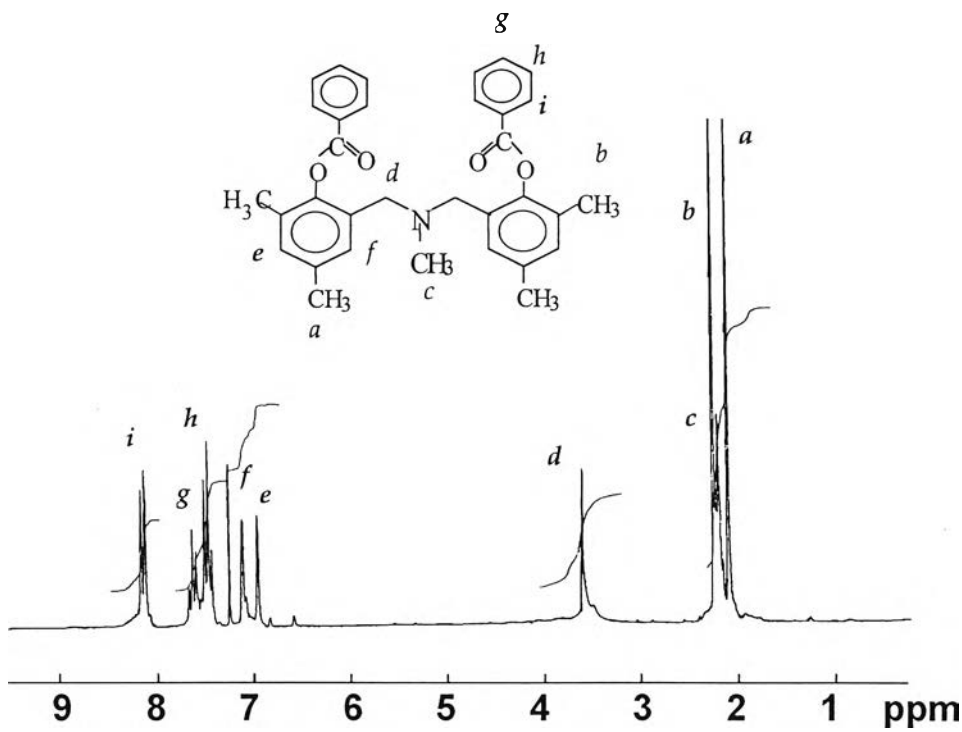

Figure 4.17 ^{1}H-NMR spectrum of (9).

4.3.4 Structural Characterization of N,N-Bis (3,5-dimethyl-2-acetyl benzyl) methylamine (10)

Yield : 80.6%. R_f (TLC, MeOH:$CHCl_3$ (1:19 v/v)) 0.94. FTIR (KBr, in cm^{-1}): 1762 (-COO-); 1451 (N-CH_3 stretching).

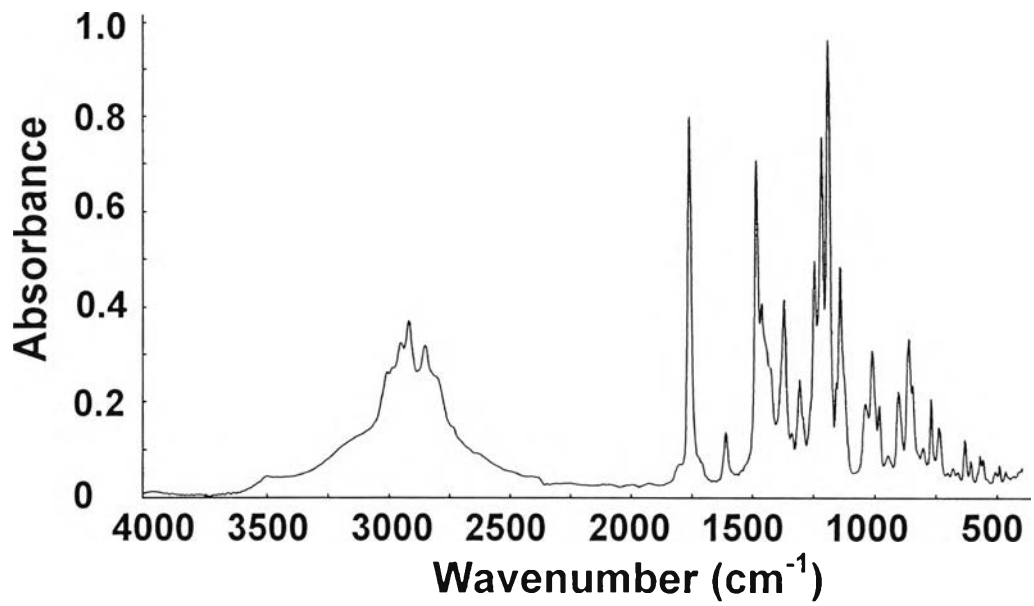

Figure 4.18 FTIR spectrum of (10).

4.3.5 Structural Characterization of N,N-Bis (5-ethyl-2-benzoyl benzyl) methylamine (11)

Yield : 89.6%. R_f (TLC, MeOH:$CHCl_3$ (1:19 v/v)) 0.97. FTIR (KBr, in cm^{-1}): 1738 (-COO-); 1452 (N-CH_3 stretching). ^{1}H-NMR (200MHz, $CDCl_3$, δ values in ppm from TMS): 1.00 (6H, t, Ar-CH2-CH3), 2.60 (3H, s, N-CH3), 2.72 (4H, m, Ar-CH2-CH3), 3.58 (4H, s, Ar-CH2-N), 6.97 (2H, d, Ar-H), 7.12 (2H, s, Ar-H), 7.12 (2H, d, Ar-H), 7.50 (4H, t, Ar-H), 7.67 (4H, t, Ar-H), 8.00 (4H, d, Ar-H).

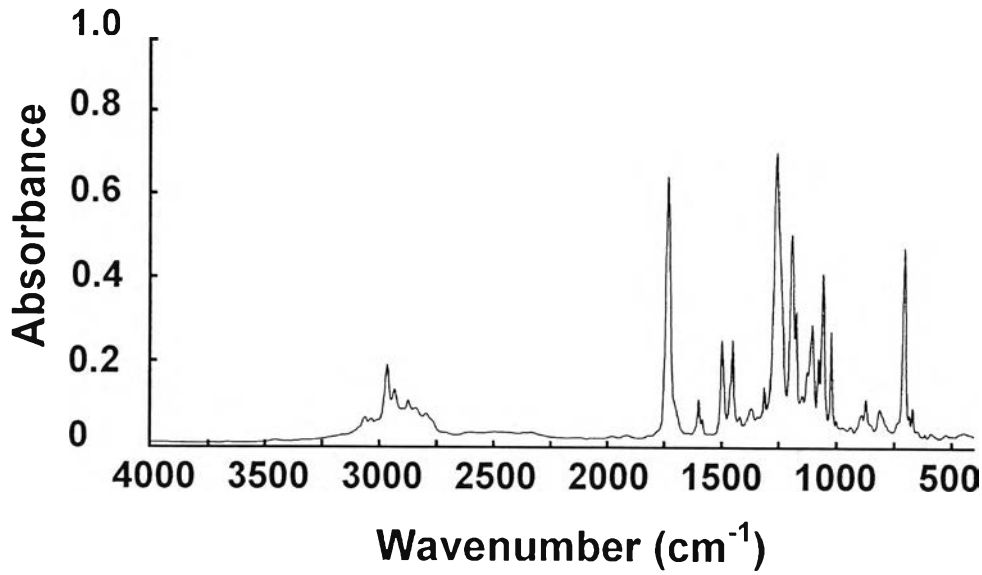

Figure 4.19 FTIR spectrum of (11).

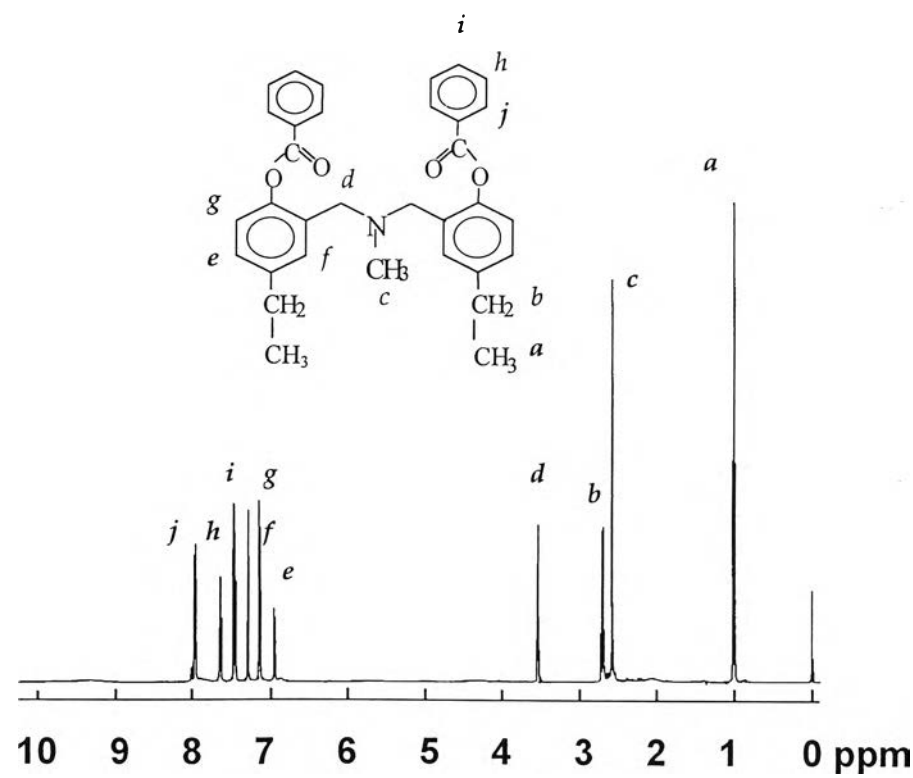

Figure 4.20 ^{1}H-NMR spectrum of (11).

4.3.6 Structural Characterization of N,N-Bis(5-ethyl-2-acetylbenzyl) methylamine (12)

Yield : 84.9%. R_f(TLC, MeOH:$CHCl_3$ (1:19 v/v)) 0.98. FTIR (KBr, in cm^{-1}): 1763 (-COO-), 1460 (N-CH_3 stretching).

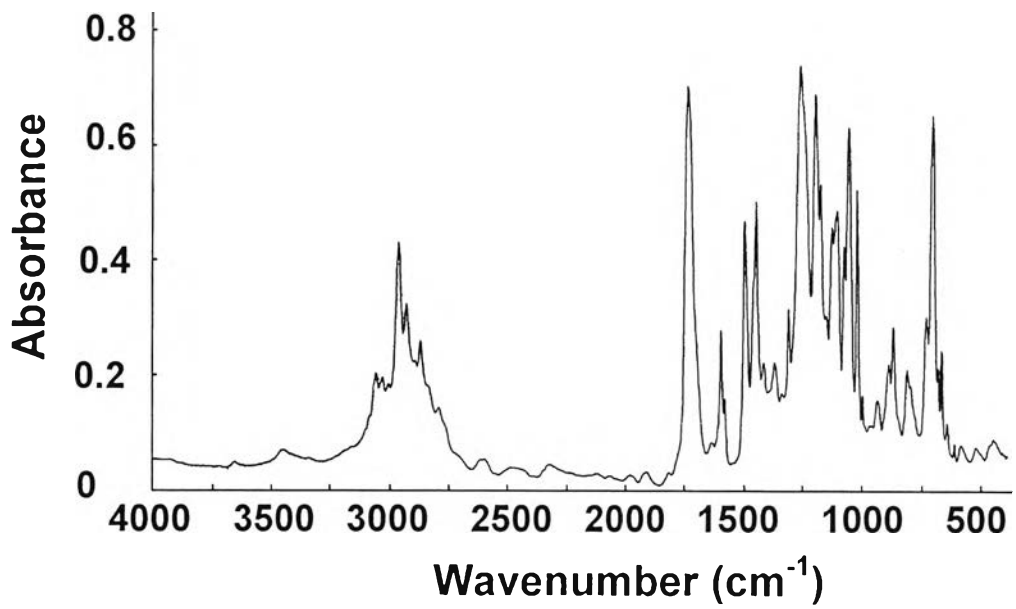

Figure 4.21 FTIR spectrum of (12).

4.4 Ion Extraction Study

By considering the structure of the obtained benzoxazines, it can be expected that benzoxazines give a specific conformation as a host compound to form complexes with some guest molecules by forming a cavity surrounding them. As known for host-guest compounds, when the guest molecules are trapped inside the host cavity, the inclusion phenomena can be distinguished by analytical techniques, such as ultraviolet spectrophotometry, infrared spectroscopy, atomic absorption spectroscopy, and nuclear magnetic resonance spectroscopy, etc.

The extraction properties were determined according to Pedersen's technique by using picrate salt extraction. The extraction results of benzoxazine dimers (4), (5), and (6) for alkaline and alkaline earth cations are summarized in Table 4.1. The extraction property of the benzoxazine dimers by varying concentration of ionophore are shown in Figures 4.22, 4.23, and 4.24. It is found that as the concentration of ionophores is increased , the extraction percentage becomes significant. Ion extraction of (4), (5), and (6) are found to be high for alkaline and alkaline earth ions. Phongtamrug *et al.* reported that, in the case of benzoxazine monomer, the steric or the bulkiness of monomer on the phenolic ring yields high efficiency on ion extraction which may be due to the loose packing structure of the molecular assembly. It should be noted that, at high concentration of (5), ion extraction percentage is found to be higher than that of (4) and (6). This also reflect that the bulky structure of (5) on the benzene ring leads to the loose packing assembly structure to entrap more amount metal ion guest entrapped inside. However, the extraction of (4), (5), and (6) shows no selectivity and all the cations are extracted to a similar extent.

Table 4.1 Extraction (%) of alkaline and alkaline earth metal picrates in $CHCl_3$ at 25^0C in various host concentration.

Guest	Ionophore								
	(4)			(5)			(6)		
	[ionophore]			[ionophore]			[ionophore]		
	$7x10^{-2}M$	$3.85x10^{-1}M$	$7x10^{-1}M$	$7x10^{-2}M$	$3.85x10^{-1}M$	$7x10^{-1}M$	$7x10^{-2}M$	$3.85x10^{-1}M$	$7x10^{-1}M$
Li	26.7	46.5	59.9	33.7	67.6	91.1	40.4	49.8	39.5
Na	34.3	46.8	59.8	47.8	73.7	87.5	44.3	50.2	67.9
K	32.9	47.2	57.7	44.3	62.6	79.8	39.7	59.2	67.5
Mg	35.9	54.7	61.7	41.6	71.9	87.3	46.6	54.8	64.1
Ca	34.4	52.0	58.8	40.0	70.5	84.5	43.3	46.1	65.7
Ba	25.6	50.4	60.0	35.1	73.5	87.4	39.1	48.6	65.0

[pic] = $7x10^{-5}M$, [MCl] = $10^{-2}M$

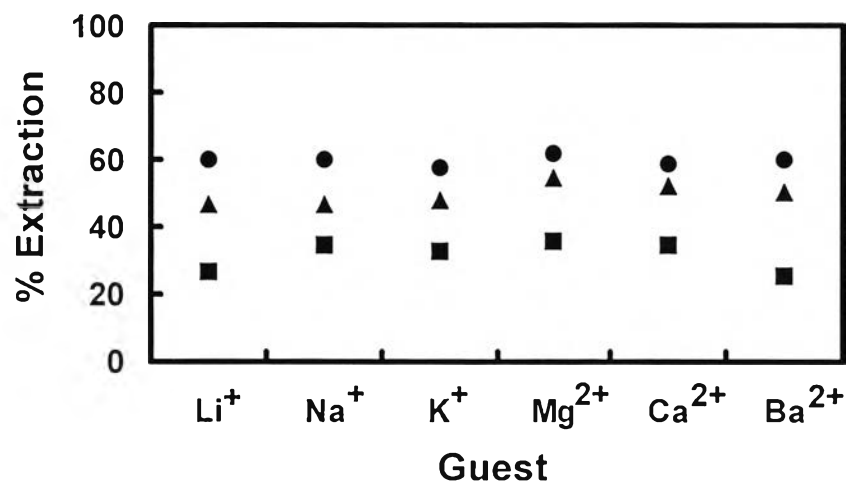

Figure 4.22 Extraction percentage of alkaline and alkaline earth metal picrates ($7x10^{-5}M$) by (4) in the concentration of, ●) $7x10^{-1}M$, ▲) $3.85x10^{-1}M$, and ■) $7x10^{-2}M$ in $CHCl_3$ at 25^0C.

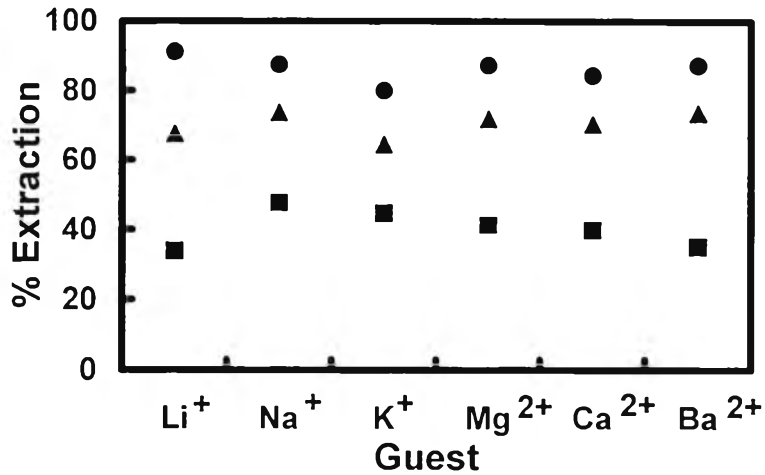

Figure 4.23 Extraction percentage of alkaline and alkaline earth metal picrates ($7x10^{-5}M$) by (5) in the concentration of, ●) $7x10^{-1}M$, ▲) $3.85x10^{-1}M$, and ■) $7x10^{-2}M$ in $CHCl_3$ at 25^0C.

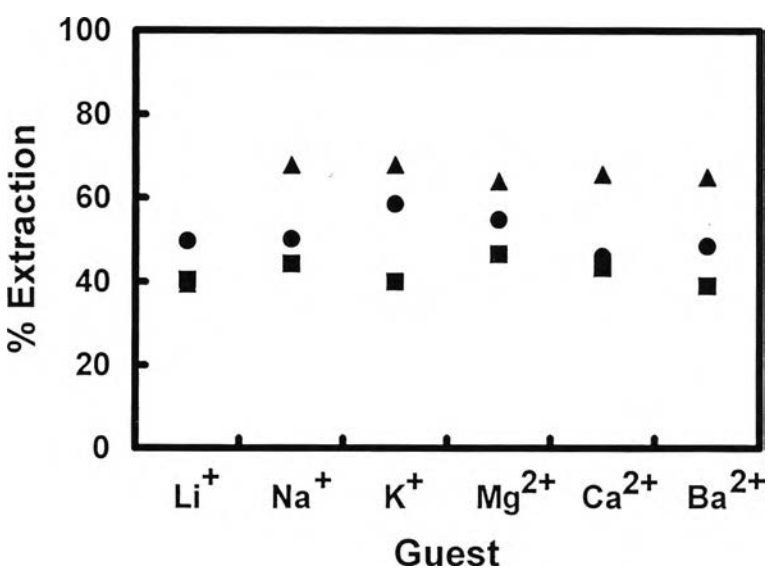

Figure 4.24 Extraction percentage of alkaline and alkaline earth metal picrates ($7x10^{-5}M$) by (6) in the concentration of, ●) $7x10^{-1}M$, ▲) $3.85x10^{-1}M$, and ■) $7x10^{-2}M$ in $CHCl_3$ at 25^0C.

In the case of benzoxazine benzoate dimer derivatives, the ion extraction ability was found to be more significant. Thus, a potassium salt was applied to compare the ion extraction ability between benzoxazine dimers (4), (5), and (6), and benzoxazine benzoate dimer derivatives (7), (9), and (11) (Figure 4.25). The ion sensitivity is found to be very high for benzoxazine benzoate type ((7), (9), and (11)) and extraction is close to 100% at $7x10^{-2}M$, which is higher than that of benzoxazine dimer ((4), (5), and (6)) by more than 100 times

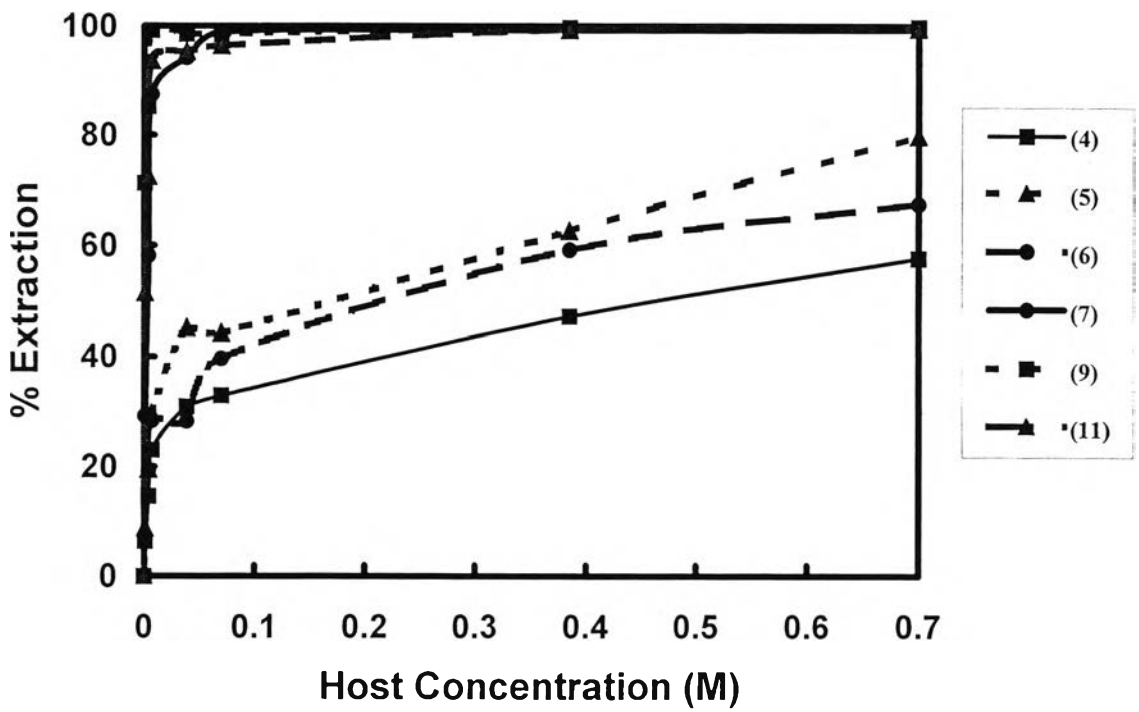

Figure 4.25 Extraction percentage of potassium picrate ($7x10^{-5}M$) by (4)-(6), (7), (9), and (11) at various concentration in $CHCl_3$ at 25^0C.

The extraction property of benzoate and acetate type benzoxazine dimer derivatives are shown in Figure 4.26, and 4.27, respectively. Here, it should be noted that the bulky groups on the benzene unit leads to the high ion extraction percentage even in the case of benzoate and acetate types of benzoxazine derivatives. This can be confirmed between the related structures of each derivative, i.e., (7) and (4), (9) and (5), and (11) and (6).

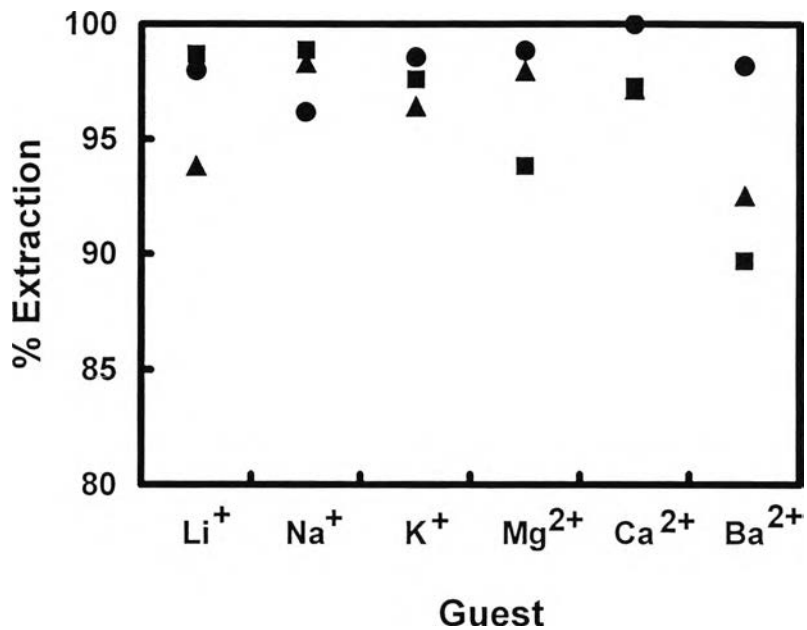

Figure 4.26 Extraction percentage of alkaline and alkaline earth metal picrates ($7x10^{-5}M$) by benzoate type benzoxazine dimer derivatives, ■ for (7),● for (9), and▲ for (11) in concentration of $7x10^{-2}M$ in $CHCl_3$ at 25^0C.

In the case of derivatives (7), (9), and (11) at the concentration of $7x10^{-2}M$, almost all metal guests at the concentration of $7x10^{-5}M$ were extracted quantitatively. As a result, the compound (9) which has the bulky

groups both on ortho and para positions show more complex affinity with metal ions than that of (7). Similarly, acetate type compounds (8), (10), and (12) give the order of extraction ability related to the effect of bulkiness on the structure.

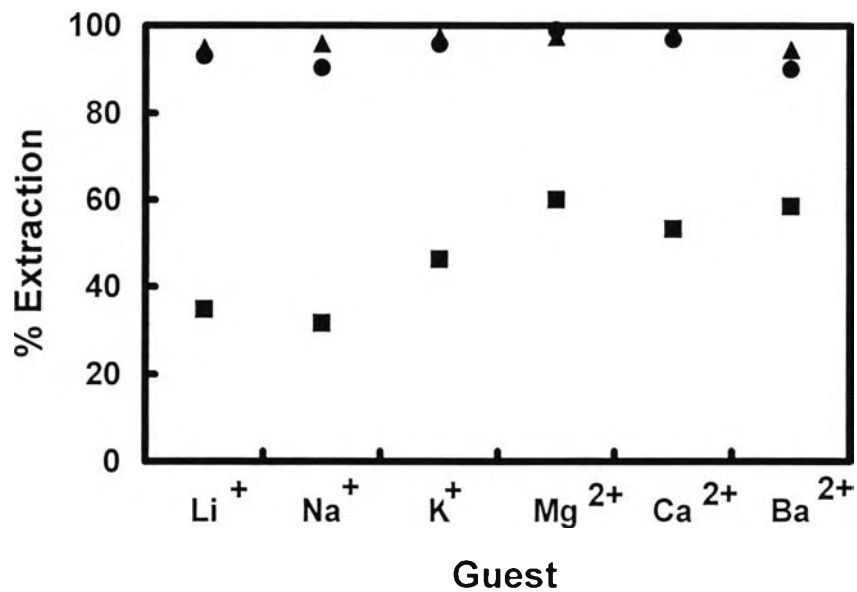

Figure 4.27 Extraction percentage of alkaline and alkaline earth metal picrates ($7x10^{-5}$M) by acetate type benzoxazine dimer derivatives, ■ for (8), ● for (10), and ▲ for (12) in concentration of $7x10^{-2}$M in $CHCl_3$ at 25^0C.

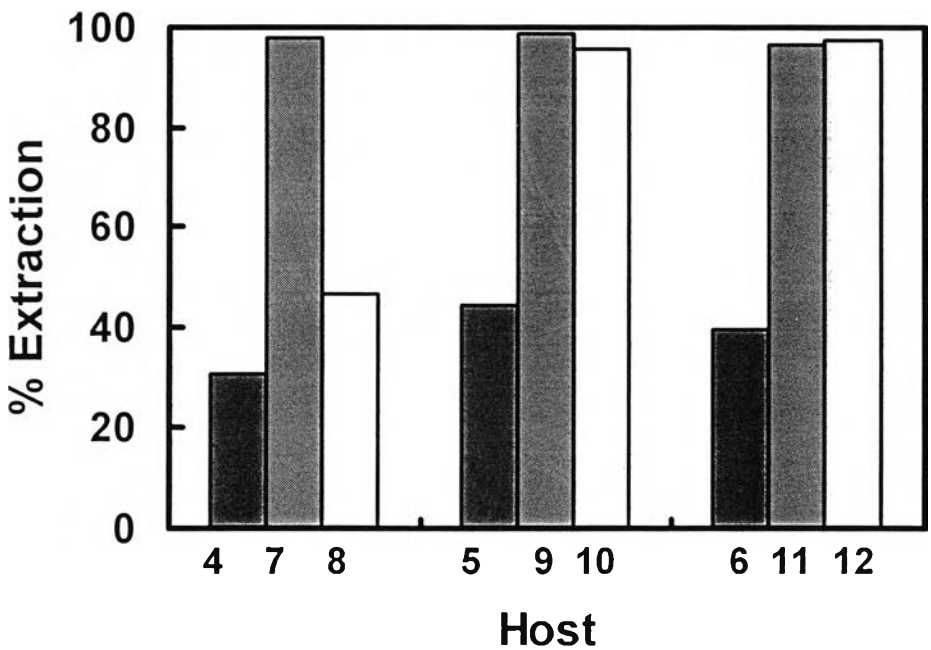

Figure 4.28 Extraction percentage of potassium picrate by benzoxazine dimer derivatives (4)-(12) in concentration of $7x10^{-2}M$ in $CHCl_3$ at 25^0C.

Figure 4.28 shows the extraction of potassium picrate by (4)-(12). The extraction studied of the ester type derivatives ((7), (9), (11)) show high ion extraction percentage than that of the normal type benzoxazine dimers ((4), (5), and (6)). This may be due to the difference of assembly formation condition. Ishida et al. reported that the opened ring benzoxazine forms intramolecular hydrogen bonding between hydroxyl group and aza group. Thus, the ability of metal guest entrapment of (4), (5), and (6) become low. In the case of ester type benzoxazine derivatives ((7)-(12)), there is no intramolecular hydrogen bonding while the ester group provides more lone pair electrons for the assembly system, and as a result metal guest entrapment is significant. When

comparing the ester type of benzoate benzoxazine dimers to acetate dimers, it is found that the former shows higher ion extraction percentage. At the moment, though the host guest structure of benzoxazine derivatives and metal ions are not clarified, the ion extraction property of benzoate type may be described as follows: benzoate type gives lone pair electrons belonging to benzene ring to interact with guest metal ions including the stacking conformation between two benzene ring in each dimer unit.

4.5 NMR Study of Complexation

^{1}H-NMR is an effective method to analyze host guest systems (D.J. Cram, 1986). Combining Pedersen's technique with ^{1}H-NMR study, the host-guest systems in this paper can be studied since metal picrate salt interacts with host compound and the complex system observed by ^{1}H-NMR will show the peak of picrate proton at a certain chemical shift.

^{1}H-NMR spectra of complexation of (7), (9), and (11) with potassium picrate (Figure 4.29, 4.30, and 4.31) show a peak of picrate proton at δ = 8.8 ppm. It should be noted that the peaks of (7), (9), and (11) are shifted and split into minor peaks. In order to determine the host-guest ratio and conformation, it is necessary to develop the study of NMR with the advanced techniques, such as 2D-NMR to determine the structure participation in the host guest system.

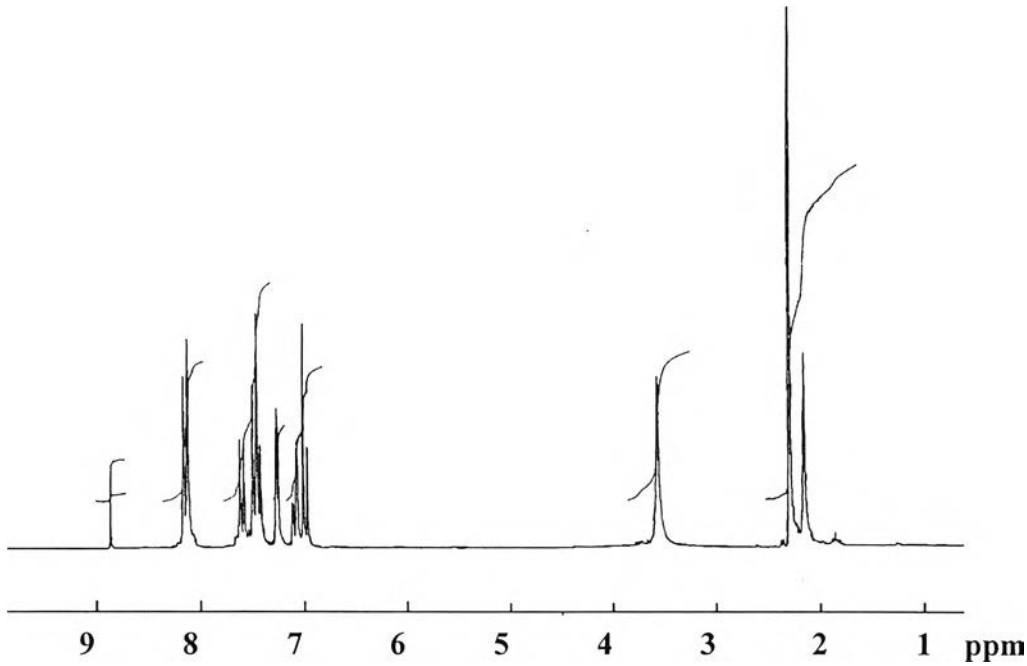

Figure 4.29 ^{1}H-NMR spectrum of complexation (7) with potassium picrate.

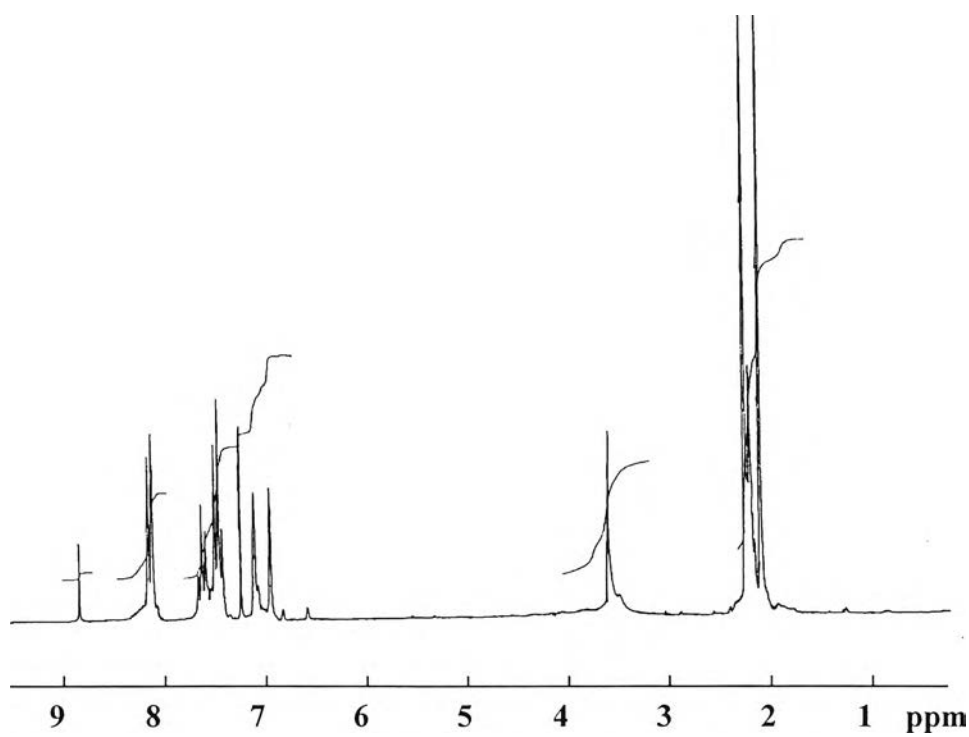

Figure 4.30 ^{1}H-NMR spectrum of complexation (9) with potassium picrate.

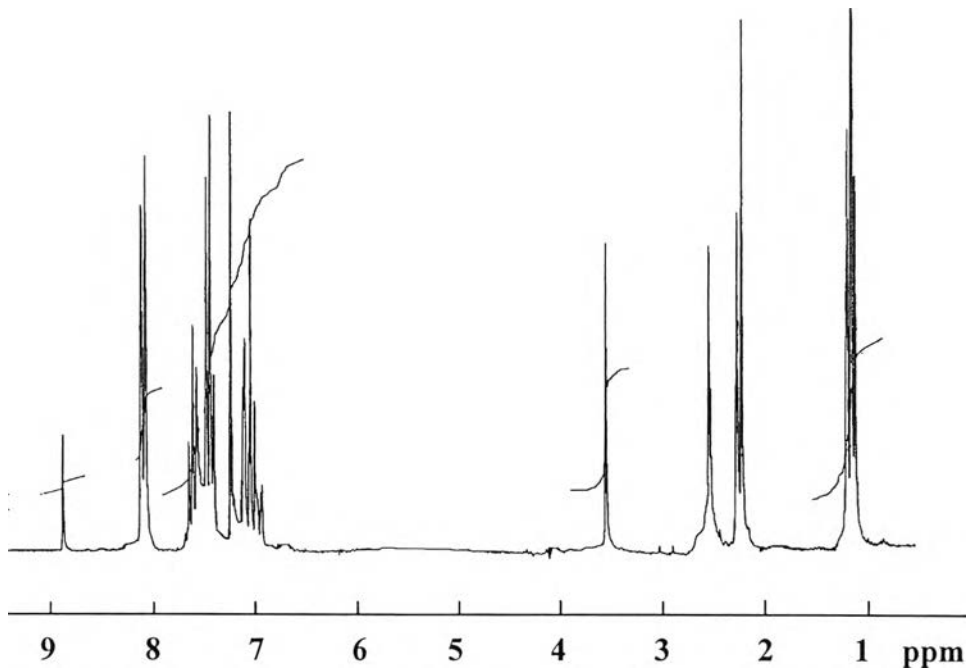

Figure 4.31 ^{1}H-NMR spectrum of complexation (11) with potassium picrate.